JMEPEG (2007) 16:663–671
DOI: 10.1007/s11665-007-9107-2

1059-9495/$19.00

Laser Cutting of Multilayered Kevlar Plates

B.S. Yilbas, F. Al-Sulaiman, C. Karakas, and M. Ahsan

(Submitted November 27, 2006; in revised form December 4, 2006)

Laser cutting of Kevlar plates, consisting of multilayered laminates, with different thicknesses are carried out. A mathematical model is developed to predict the kerf width, thermal efficiency, and specific energy requirements during cutting. Optical microscopy and Scanning Electron Microscopy (SEM) are employed to obtain the micrographs of the cutting sections. The kerf width size is measured and compared with the predictions. A factorial analysis is carried out to assess the affecting parameters on the mean kerf width and dimensionless damage sizes. It is found that the kerf width and damage sizes changes sharply when increasing cutting speed from 0.03 to 0.08 m/s. Thermal efficiency of the cutting process increases with increasing thickness and cutting speed while specific energy reduces with increasing thickness. The main effects of cutting parameters are found to be significant on the mean kerf width and dimensionless damage sizes, which is more pronounced for the workpiece bottom surface, where locally distributed char formation and sideways burning are observed.

Keywords cutting, Kevlar, laser, multilayer

Nomenclature

A	area (m^2)
A_e	energy coupling factor, <1
C_p	specific heat at constant pressure (J/kgK)
C_{p_e}	equivalent specific heat at constant pressure (J/kgK)
C_{p_f}	specific heat at constant pressure for fiber(J/kgK)
C_{p_a}	specific heat at constant pressure for void (J/kgK)
C_{p_r}	specific heat at constant pressure for resin (J/kgK)
d	kerf depth (m)
$\dot{E}_T$	rate of energy required for through hole drilling (W)
$\dot{E}_{Conduction}$	rate of conduction energy loss (W)
$\dot{E}_{Convection}$	rate of convection energy loss (W)
f	fraction of pressure drop in the kerf, <1
h_1	Heat transfer coefficient at upper surface of the plate (W/m^2K)
h_2	Heat transfer coefficient at bottom surface of the plate (W/m^2K)
h	heat transfer coefficient (W/m^2K)
k	thermal conductivity (W/mK)
L	length of cut (m)
L_b	latent heat of evaporation (J/kg)
L_m	latent heat of melting (J/kg)
L_o	total length of cut (m)
M_w	molecular weight of assisting gas (g/mol)
P	power input in the workpiece (W)
P_0	power input at the workpiece surface (W)
t	time (s)
T	temperature (K)
T_a	ambient temperature (K)
T_m	melting temperature (K)
T_o	initial temperature (K)
T_{us}	upper surface temperature (K)
T_{bs}	bottom surface temperature (K)
T_∞	temperature for away from hole (K)
T_h	workpiece thickness (m)
u	laser cutting speed (m/s)
v	laser beam cutting speed (m/s)
V_f	volume fraction of fiber
V_r	volume fraction of resin
V_v	volume fraction of void
w	laser beam waist diameter at workpiece surface (m)
w_k	kerf width (m)
w_0	beam waist diameter at surface when focus setting is nominal (m)
x	axial distance (m)
y	tangential distance (m)
z	vertical distance (m)

Greek

α	thermal diffusivity (m^2/s)
β	fraction of evaporation contribution, <1
σ	the molecular diameter (Å)
η_u	super heating factor in the melt front, <1
ρ	density of workpiece material (kg/m^3)
ρ_a	density of void (kg/m^3)
ρ_e	equivalent density (kg/m^3)
ρ_f	density of fiber (kg/m^3)
ρ_r	density of resin (kg/m^3)
ρ_g	density of assisting gas (kg/m^3)
$\forall$	volume (m^3)

B.S. Yilbas, F. Al-Sulaiman, and **M. Ahsan,** ME Department KFUPM, Dhahran 31261, Saudi Arabia; and **C. Karakas,** Engineering Faculty, Hacettepe University, Ankara, Turkey. Contact e-mail: bsyilbas@kfupm.edu.sa.

1. Introduction

Laser cutting of multilayer composites has several advantages over the conventional cutting techniques. Some of the

important advantages are achievement of good end product quality, short processing time, and low-specific energy requirements for the cutting process. This is particularly true for multilayered Kevlar plates; in which case, conventional cutting techniques result in whiskers formation around the cutting edges. In laser cutting process, the end product quality and specific energy requirements depend on the laser and workpiece parameters. Some of the parameters include, laser output power, duty frequency, cutting speed, assisting gas type, and its pressure, focus setting of a laser power intensity, and workpiece thickness. The proper selection of these parameters results in improved end product quality. The cut quality can be assessed through variation in kerf width size and out of flatness along the cut sections (Ref 1). Consequently, investigation into effect of each process parameter on the kerf width variation and damage sizes along the cut sections becomes essential.

Considerable research studies were carried out to examine laser processing of composites. Thermal conductivity of unidirectional fiber-reinforced plastics in relation to laser machining was evaluated by Pan and Hocheng (Ref 2). They showed that laser processing resulted in a steep temperature gradient in the vicinity of the kerf. Effects of heat treatment on the mechanical properties of Kevlar-29 fiber were examined by Yue et al. (Ref 3). They showed that the Young's Modulus of the single fiber was not affected by heat treatment and heat treatment in vacuum did not have any effect on the tensile strength of the fiber. A comparative study on the effect of Kevlar fiber reinforcement on the thermal and dynamic properties of composite was carried out by Tandon et al. (Ref 4). They showed that reinforcement by Kevlar fibers had a catalytic effect on the curing reaction and when the Kevlar content increased, the heat-flow curves and the exothermic peak temperature shifted significantly to lower temperatures. Laser drilling of blind holes in Kevlar and glass/epoxy composites for multilayer printed wiring boards were carried out by Hirogaki et al. (Ref 5). They showed that using lasers reduced the fabrication time significantly and the surface roughness on the sidewalls of the hole was smaller with Kevlar than a glass/epoxy composite. Laser cutting of Aramid fiber reinforced plastics was investigated by Di Ilio and Tagliaferri (Ref 6). They examined the features of the laser cut edges using a digital image processing technique. Structural changes in thermally enhanced Kevlar-29 fiber were examined by Downing and Newell (Ref 7). They indicated that heat treatment of Kevlar-29 fiber resulted in cross-linking of its skin region and hydrogen-bond disruption within the core reaction. Heat of combustion of high-temperature polymers was examined by Walters et al. (Ref 8). They used a bomb calorimeter technique and tabulated heat of combustion of various composites including Kevlar. Tagliaferri et al. (Ref 9) examined laser cutting of fiber-reinforced composites. They assessed the end product quality and indicated that laser-cutting parameters had significant effect on the end product quality, in particular cutting speed and laser output power. Chen and Cheng (Ref 10) studied laser processing of composites. They evaluated the material properties in relation to laser cutting parameters and indicated that the predictions for heat effect zone were in good agreement with the experimental results. Cenna and Mathew (Ref 11) investigated laser cutting of fiber-reinforced polyesters. They showed that structural integrity in the matrix of the material as well as thermal properties were the main concerns affecting the end product quality. Yilbas (Ref 12), Al-Sulaiman and Yilbas (Ref 13), and Al-Sulaiman et al. (Ref 14) examined laser cutting of plastic, carbon, and composites. They indicated that laser output power, assisting gas pressure, and cutting speed influenced significantly the end product quality.

In the present study, laser cutting of multilayer Kevlar plates is carried out for different laser cutting conditions. Mathematical analysis is introduced for the kerf width predictions. Specific energy requirements for each cutting conditions is computed and compared with its counterpart obtained from the conventional cutting methods. The end product quality is assessed using the international standards for thermal cutting. A statistical analysis using a factorial design is carried to assess the affecting process parameters on the kerf width and damage sizes.

2. Experimental

The equipment used and the experimental procedure and conditions are given below under the appropriate subheadings.

2.1 CO_2 Laser System

A CO_2 laser system (LC-αIII-Amada) delivering nominal output power of 2000 W at pulse mode width different frequencies are used in the experiment. Nitrogen is employed as an assisting gas, emerging from a conical nozzle and coaxially with the laser. A nominal focal length of 127 mm lens with defocusing facilities is used to focus the laser beam onto the workpiece surface. The laser cutting parameters are given in Table 1.

2.2 Scanning Electron Microscopy (SEM) and Optical Microscopy

The cut surfaces and cross sections are examined using JEOL JDX-3530 scanning electron microscope (SEM), while a digital camera (PIXERA) was used for optical photography.

2.3 Kevlar Plate

Kevlar plate consists of laminates, which is multilayer plain weave polyester at different uniform thicknesses. The fiber/resin volume ratio is varied to obtain difference thicknesses of the laminate. The calculation of thermal properties of the laminate is given in (Ref 15, 16). Table 2 gives the properties of Kevlar plate used in the simulations and the cutting experiments. The laminate was prepared by the multistep heat treatment process. The initial preparation of the laminate was carried out at 8 bar pressure and 175 °C for 2 h. The workpieces were then heated to 1000 °C in an argon environment for several hours to ensure the conversion of the phenolic matrix into carbon, at the same time monitoring the density.

Table 1 Laser cutting parameters

Feed rate, m/s	Power, W	Frequency, Hz	Nozzle gap, mm	Nozzle diameter, mm	N_2 pressure, kPa
0.005-0.67	500-2000	100-300	1.5	1.5	600

Table 2 Properties of Kevlar at different thicknesses

Thickness, mm	Equivalent density, g/cm^3	Fiber volume fraction	Resin volume fraction	Air voids volume fraction	Equivalent thermal conductivity, J/(m·K)	Equivalent specific heat, J/(g·K)	Equivalent thermal diffusivity, m^2/s
11.970	0.8995	0.3318	0.3318	0.3365	0.2221	1.913	1.29E-07
8.057	1.135	0.4186	0.4186	0.1628	0.1658	1.913	7.64E-08
8.610	1.17	0.4317	0.4317	0.1365	0.1573	1.913	7.03E-08
7.023	1.23	0.4540	0.4540	0.09197	0.1430	1.914	6.07E-08
6.653	1.284	0.4736	0.4736	0.05273	0.1306	1.914	5.32E-08
6.76	1.342	0.4952	0.4952	0.009663	0.1202	1.914	4.68E-08
4.50	1.342	0.4952	0.4952	0.009663	0.1202	1.914	4.68E-08
3.80	1.342	0.4952	0.4952	0.009663	0.1202	1.914	4.68E-08
2.80	1.342	0.4952	0.4952	0.009663	0.1202	1.914	4.68E-08

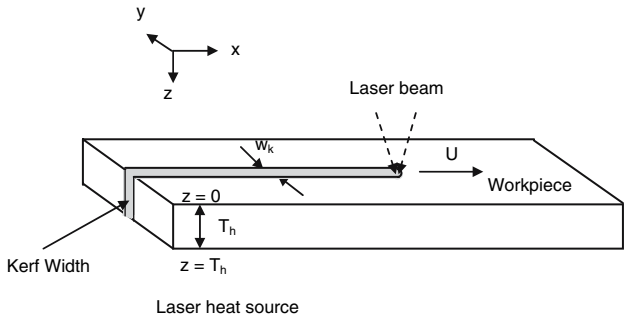

Fig. 1 Laser cutting and geometric configurations of cut section

When the density of the workpiece had reached a certain value, the process was stopped.

3. Mathematical Formulation

The mathematical analyses are given under the subheadings.

3.1 Specific Energy Requirement

The specific energy required for a laser cutting into Kevlar plate is formulated using a lump parameter technique. In this case, the rate of energy balance for cutting of a plate is considered in the formulations. The cutting situation and geometric view of the hole is shown in Fig. 1.

The rate of energy required ($\dot{E}_T$) for cutting of the plate can be written as:

$$\dot{E}_T = \dot{E}_l + \dot{m}[\Delta u + L_m + \beta L_{ev}], \quad \text{(Eq 1)}$$

where $\dot{E}_l$, $\dot{m}$, Δu, L_m, β, L_{ev} are the rate of total losses during the cutting, the rate of total mass of material removed during laser cutting, internal energy gain of the substrate material removed, latent heat of melting, fraction of mass evaporated, latent heat of evaporation, respectively.

The total material removed during laser cutting, after assuming a uniform density of the substrate material, is:

$$\dot{m} = \rho \frac{d\forall}{dt} = \rho \frac{d(w_k L T_h)}{dt} = \rho w T_h \frac{dL}{dt} = \rho w T_h U \quad \text{(Eq 2)}$$

where $\forall$ is the volume of the laser cut hole, ρ is the density of the substrate material, w_k is the kerf width, L is the cut length, T_h is the thickness of the plate, and U is the cutting speed.

In addition, the rate of total loss includes the rate of conduction and convection losses during the drilling, i.e.:

$$\dot{E}_{loss} = \dot{E}_{conduction} + \dot{E}_{convection} \quad \text{(Eq 3)}$$

where $\dot{E}_{conduction}$ and $\dot{E}_{convection}$ are the rate of conduction and convection losses.

It is assumed that the natural convection occurs at the top and bottom surfaces of the cut section. The heat transfer coefficients across both surfaces are the same. In this case, the convection losses can be written as:

$$\begin{aligned} \dot{E}_{convection} &= A_s[h_1(T_s - T_o) + h_2(T_s - T_o)] \\ &= w_k L_o (T_s - T_o)(h_1 + h_2), \end{aligned} \quad \text{(Eq 4)}$$

where A_s (= $w_k L_o$) is the surface area of the cut section, L_o is the total cut length, h_1 and h_2 are the heat transfer coefficient at the top and bottom surfaces of the cut section.

To determine the heat conduction losses, the heat conduction equation should be solved to obtain temperature distribution inside the substrate material next to the cut edge. Transient heat conduction equation pertinent to heating situation can be written as:

$$k\left[\frac{\partial^2 T}{\partial x^2} + \frac{\partial^2 T}{\partial y^2} + \frac{\partial^2 T}{\partial z^2}\right] = \rho C_p \frac{\partial T}{\partial t}. \quad \text{(Eq 5)}$$

Initially it is assumed that the workpiece material is at uniform constant temperature (T_o), i.e.:

$$\text{At } t = 0 : T = T_o.$$

At the upper and lower surfaces (limited with $z = 0$ to $z = T_h$ and $y = w_k$) of the workpiece, convective boundaries are assumed. Therefore, the boundary condition at the upper surface is:

$$k\frac{\partial T}{\partial z} = h_1(T_{us} - T_\infty),$$

where T_{us} is the upper surface temperature.

Similarly, the bottom surface boundary condition is:

$$k\frac{\partial T}{\partial z} = h_2(T_{bs} - T_\infty),$$

where T_{ub} is the bottom surface temperature.

At kerf wall temperature is assumed to be uniform at melting or charring temperature of the workpiece material, i.e.:

$$\text{At } y = -w_k/2 \text{ and } y = w_k/2 : z = 0 \text{ to } z = T_h \rightarrow T = T_w,$$

where T_w is the hole wall temperature.

At infinitely large distance in the y direction, it is assumed that temperature is constant (T_o), i.e.:

$$\text{At } y = \infty,\ z = 0 \text{ to } z = T_h \rightarrow T = T_o.$$

Equation 5 is used numerically using an implicit scheme. However, the grid independency test was carried out and grid satisfying the grid independent solution is selected. In this case, the grid selected has $80 \times 40 \times 15$ mesh points in the x, y, and z-axes, respectively.

The specific energy required for the cutting is determined from:

$$E_{spec} = \frac{1}{w_k L_o T_h} \int_o^{t_c} \dot{E_T} dt, \qquad \text{(Eq 6)}$$

where t_c is the time taken to complete the length L_o of cut in the laminate.

3.2 Thermal Efficiency

Thermal efficiency of the laser drilling process is the ratio of rate of energy required for through hole drilling over the power used for drilling. In this case, thermal efficiency becomes:

$$\eta = \frac{\dot{E}_{req}}{P}. \qquad \text{(Eq 7)}$$

The solution of Eq 1-6 and 7 are solved using Mathematica software. The data used in the solution are given in Table 2 and 3.

3.3 Formulation of Kerf Width

The energy balance for cutting process can be used to formulate the kerf width size during laser cutting process. The simplified relation based on the scaling law analysis can yield (Ref 17).

$$\frac{P}{d} = \frac{v w_k + A_3 \sqrt{v w_k}}{A_0}, \qquad \text{(Eq 8)}$$

P is the laser output power and d is the spot diameter at the workpiece surface. A_0 and A_3 are:

$$A_0 = \frac{A_e}{a_0} \text{ and } A_3 = \frac{1}{a_0} \frac{(w_k + 2w_k(T_m - T_0))}{2\sqrt{\alpha w w_k}}, \qquad \text{(Eq 9)}$$

where A_e is the coupling factor and a_0 is:

$$a_0 = \rho\left(C_p(T_m - T_0) + L_m + \beta L_b\right), \qquad \text{(Eq 10)}$$

where w_k is the kerf width, w the laser beam waist size, l the length of the cut, T_m the melting temperature of the substrate material, T_o the ambient room temperature. β is the contribution of evaporation of the surface.

Applying scaling law for the laser cutting process and after the mathematical arrangements kerf width size can be written as (Ref 17):

$$w_k = \frac{1}{v}\left[\frac{2.51\sqrt{\frac{\alpha}{w}}\frac{(2A\eta_u)}{k(T_m - T_0)} P\sqrt{v}}{1 + 3.08 \times 10^7 \left(\frac{A_0}{A_3\sqrt{f}}\right)\left(\frac{\rho\rho_g\sigma^2\alpha}{M_w P_g f\sqrt{w}}\right) P\sqrt{v}}\right], \qquad \text{(Eq 11)}$$

Table 3 Properties used in the simulations

Source of variation	Value	Units
Density of assisting gas	2.786	kg/m^3
Fraction of evaporation contribution (β)	0.1	...
Fraction of pressure drop (f)	0.5	...
Energy coupling factor (A)	0.6	...
Super heating factor in the melt front (η_u)	0.01	...
Heat of reaction	26.92×10^3	J/kg
Molecular diameter of nitrogen	0.3176	Å
Specific heat capacity of workpiece	1400	J/kgK
Superheating factor	0.02	...

where f is the fraction of pressure drop in the kerf, σ the molecular diameter (Å, Angstrom unit), M_w the molecular weight (g/mol unit) of the assisting gas, P_g and ρ_g the pressure and density of the assisting gas, and η_u the superheating factor in the melted zone.

The kerf width size is determined from Eq 11 using the Mathematica Software Package. Table 3 gives the properties used in the simulations. It should be noted that the latent heat of melting is replaced with the heat of reaction, since the combustion is the major process for mass removal from the kerf during the cutting.

3.4 Factorial Analysis

To analyze the effect of laser cutting parameters on the resulting damage size, it is necessary to design an experiment in such a way that the influence of each parameter could be examined individually with an interaction. This requires a complete factorial design in which selected factors are varied at appropriately selected levels. The percentage of damage size can be estimated by the ratio of damage size around the cut edges to the kerf width size of the corresponding cut, i.e.:

$$\%\,\text{Damage size} = \frac{\Delta w_k}{w_k},$$

where Δw_k is the damage size or enlargement/contraction of the kerf width after cutting and w_k is the kerf width size. It should be noted that damage size and kerf width were measured using an optical microscopy and each measurement were repeated three times to ensure the repeatability of the results.

In statistical analysis, the qualitative factors are nonordered, i.e., each level is of intrinsic interest (Ref 18). The mathematical analyses of factorial design are not given here, but refer to (Ref 19). It should be noted that in the qualitative analysis, main effects are zero order effects, i.e., independent of each other. However, first order interactions demonstrate that the effects of the interacted factors on observation are dependent on each other. The affecting factors can be stated as: Laser power, Cutting speed, and Pulse frequency, which have the main effects while the first order interactions of the affecting parameters are: Laser power × Cutting speed, Laser power × Pulse frequency, and Cutting speed × Pulse frequency.

An F test is conducted to identify the significant effects of the parameters and their interactions on the various observations describing the cut quality. The terms most significant, very significant, and significant refer to minimum correlation levels of 0.99, 0.99-0.95, and 0.95-0.90 of the factors, respectively.

4. Results and Discussions

Laser cutting of Kevlar plates is carried out and thermal efficiency, kerf width, specific energy requirements for cutting are formulated and predicted for various cutting parameters. Statistical analysis for the end product quality assessment is carried out and the affecting cutting parameters for the cut quality are identified. The structure of the cut surfaces are examined using SEM and EDS is employed to identify the oxygen content on the cut sections.

Figure 2 shows thermal efficiency with plate thickness for various cutting speeds and laser output powers. Thermal efficiency increases with increasing thickness and cutting speed. This is more pronounced for low-laser power settings. In this case, energy required for mass removal from the cut section increases with increasing thickness. Consequently, laser power absorbed by the substrate material is used at a high percent for mass removal from the cut section, i.e. percentage of excessive laser power reduces during the cutting process. This, in turn, increases the thermal efficiency. Moreover, increasing laser scanning speed enhances the thermal efficiency. This is because of the mass removal rates, which improves at high-laser scanning speed. Some small irregular variation in thermal efficiency occurs between the workpiece thicknesses of 7-9 mm, which is because of the variation of the thermal properties of plate in this thickness range. This can be seen from Table 2.

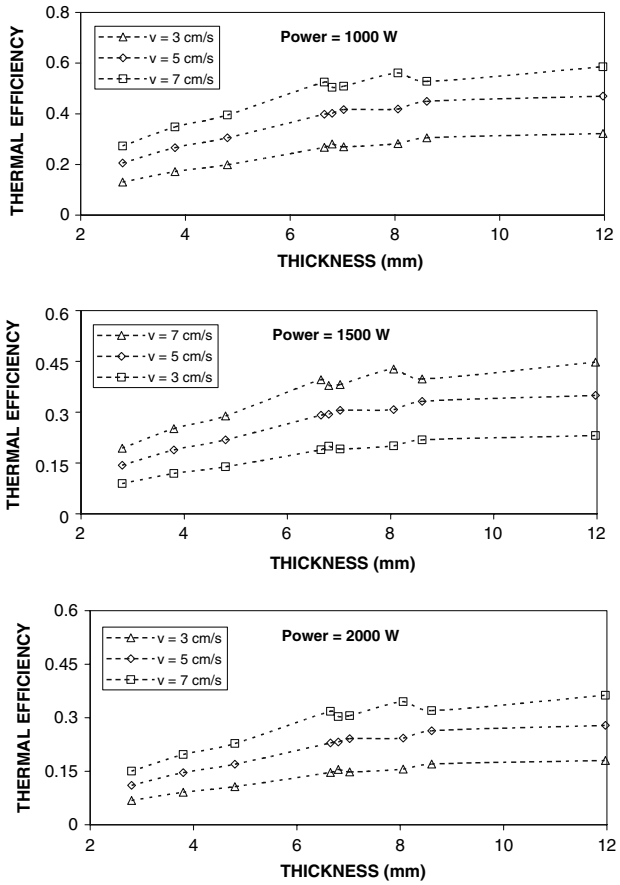

Fig. 2 Thermal efficiency of laser with workpiece thickness for different cutting speeds and laser output power

Figure 3 shows kerf width variation with laser scanning speed, kerf width size varies sharply for scanning speeds in the range of 0.03-0.08 m/s. However, increasing scanning speed beyond 0.08 m/s, kerf width size decays monotonically. This is because of the laser irradiated energy available in the cutting section; in which case, sideways burning enhances the kerf width. It should be noted that laser irradiated energy across the focused spot increases as the scanning speed reduces; consequently, radial conduction and sideways burning in the kerf section increases the kerf size. In addition, this increases the surface roughness of the cut surface as evident from Fig. 4, in which surface roughness profiles of the cut surfaces is shown. Since the Kevlar plate is formed by layers of laminates with different fiber orientations. Since the cutting direction is normal to the laminate surface, smooth cut surface is difficult to achieve. In the case of low scanning speed this situation worsens. When comparing the experimental data with the predictions, it can be observed that predictions agree well with the experimental data. It should be noted that experimental error is estimated as about 7.5%.

Figure 5 shows percentage of damage size with plate thickness for different duty cycles of the laser pulse. The damage size is within the order of 0.8% of the kerf width size, which is considerably small. The variation of percentage of damage size with plate thickness is rather random, which is true for all duty cycles. This indicates that the effect of duty cycles on the variation of percentage of damage size with thickness is not significant. Consequently, no simple functional relation can be introduced between percentage of damage size and workpiece thickness regardless of the duty cycle. Increasing laser pulse frequency results in slight increase in the percentage of the damage size. The slight increase in percentage of damage size indicates that high pulsing frequency results in the sideways burning and enhances heat conduction normal to the cutting axis in the cutting section, unlike metals (Ref 20). High-temperature combustion in the kerf section increases the kerf width size and the percentage of damage size, i.e., size of the plume generated in the cutting section increases.

Figure 6 shows the specific energy with plate thickness as predicted from Eq 6. Specific energy requirement reduces with increasing thickness, provided that the variation is in parabolic form. The specific energy requirement is significantly less than that corresponding to the conventional cutting methods (Ref 21). Consequently, laser process does not only provide processing and precision of operation as well as lowers the specific energy consumed during the cutting process. The

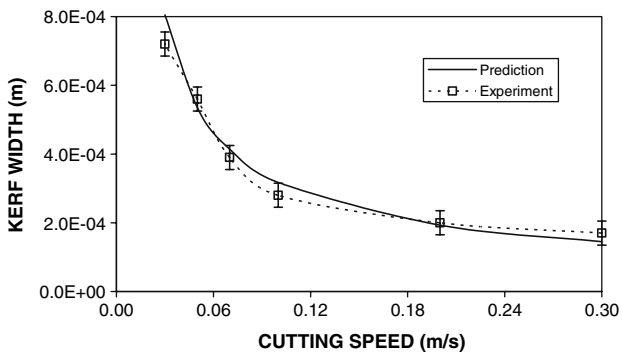

Fig. 3 Kerf width with laser cutting speeds predictions and experimental results

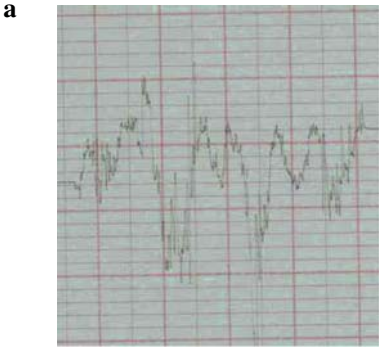

Cutting Speed = 25 cm/s: Laser Power = 2000 W: Frequency = 100 Hz: Duty Cycle = 0.40

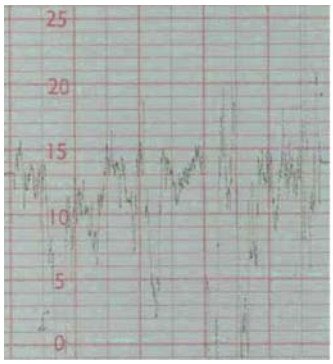

Cutting Speed = 3 cm/s: Laser Power = 2000 W: Frequency = 100 Hz: Duty Cycle = 0.40

Fig. 4 Surface roughness of the kerf side. (a) Cutting Speed = 25 cm/s: Laser Power = 2000 W: Frequency = 100 Hz: Duty Cycle = 0.40; (b) Cutting Speed = 3 cm/s: Laser Power = 2000 W: Frequency = 100 Hz: Duty Cycle = 0.40

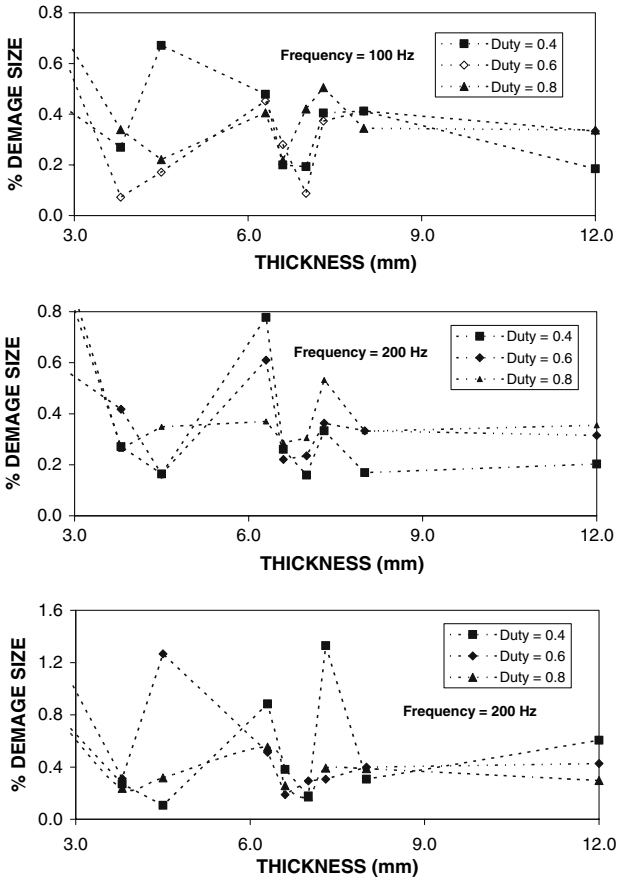

Fig. 5 Percentage of kerf width damage with workpiece thickness for different frequency and duty cycle

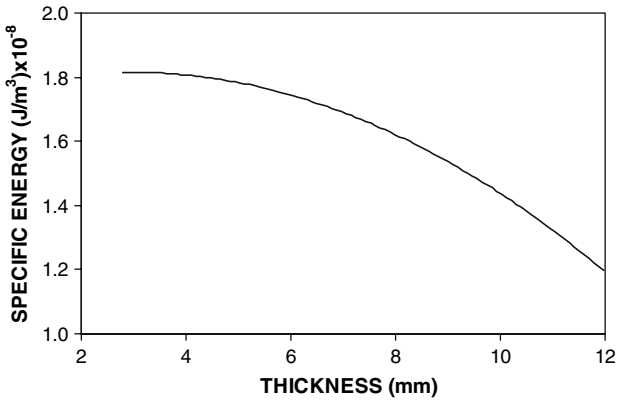

Fig. 6 Specific energy predicted for different workpiece thicknesses

reduction in the specific energy requirements with increasing plate thickness is associated with the volume of material removed from the cutting section. Consequently, increasing the volume of material removed from the kerf site lowers the specific energy requirements, provided that further increase in the volume of material removed from the cutting section results in poor-cutting quality.

Table 4 gives *F*-test results for mean kerf width size and dimensionless kerf width damage size. It is observed from the *F*-test results that main effects of laser output power and cutting speed have very significant effect on the mean kerf width size. However, pulse frequency has only significant effect on the mean kerf width size. This indicates that the mean kerf width size changes with changing of these parameters, provide that this change becomes more pronounced with changing laser output power and cutting speed as compared to laser pulse frequency. Consequently, the mean kerf width size is sensitive to the changes of laser output power and cutting speed. This is because of the power available at the surface, which is associated with the material removal rate from the cutting section; in which case, increasing laser output power increases the mean kerf width size. In addition, lowering the cutting speed enhances the laser irradiated energy intensity in the cutting section. Therefore, the mean kerf width size increases. The first order interaction of laser output power and cutting speed is significant, which in turn indicates that the coupling of laser output power and cutting speed has significant effect on the mean kerf width size. This situation is associated with energy intensity available in the cutting section for material removal, which increases with reduced cutting speed and increased laser output power. In the case of dimensionless kerf width damage size, the laser output power, cutting speed, and pulse frequency have a significant effect at the top and bottom surfaces of the workpiece. This indicates that increasing laser power while lowering cutting speed enhances the energy intensity at the cutting section and damage size increases due to excessive heating situation. The first order interactions of

Table 4 *F*-test results for the parameters used in the experiments

Source of variation	Mean kerf width	Percentage of damage size	
		Top surface	Bottom surface
Laser output power	0.95	0.95	0.95
Cutting speed	0.95	0.95	0.95
Pulse frequency	0.90	0.90	0.95
Laser out power × cutting speed	0.90	0.90	0.95
Laser out power × pulse frequency	<0.90	<0.90	0.90
Pulse frequency × cutting speed	<0.90	<0.90	<0.90

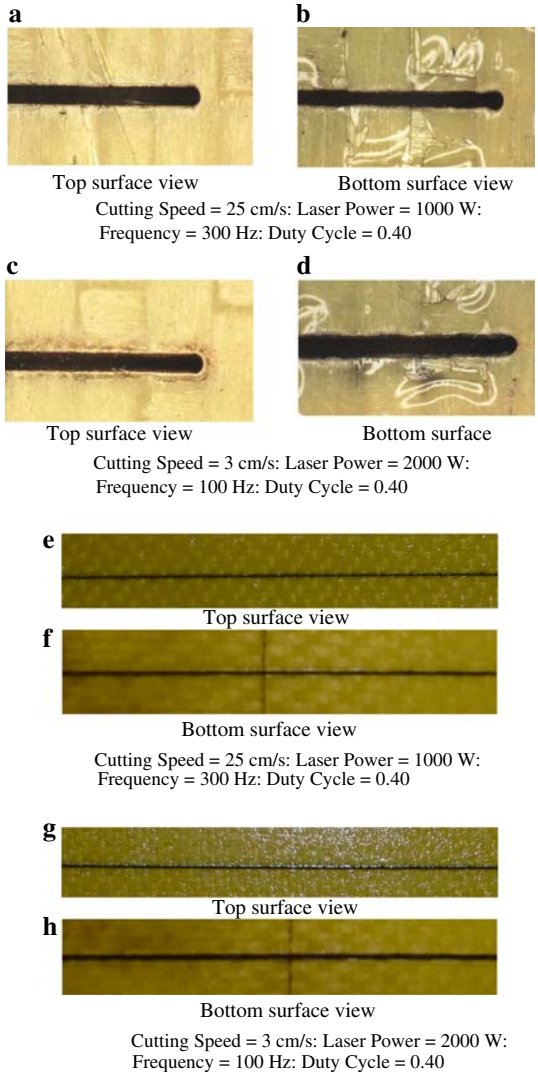

Fig. 7 Photographs of laser cut surfaces. (a) Top surface view; (b) Bottom surface view; Cutting Speed = 25 cm/s: Laser Power = 1000 W: Frequency = 300 Hz: Duty Cycle = 0.40; (c) Top surface view; (d) Bottom surface; Cutting Speed = 3 cm/s: Laser Power = 2000 W: Frequency = 100 Hz: Duty Cycle = 0.40; (e) Top surface view; (f) Bottom surface view; Cutting Speed = 25 cm/s: Laser Power = 1000 W: Frequency = 300 Hz: Duty Cycle = 0.40; (g) Top surface view; (h) Bottom surface view; Cutting Speed = 3 cm/s: Laser Power = 2000 W: Frequency = 100 Hz: Duty Cycle = 0.40

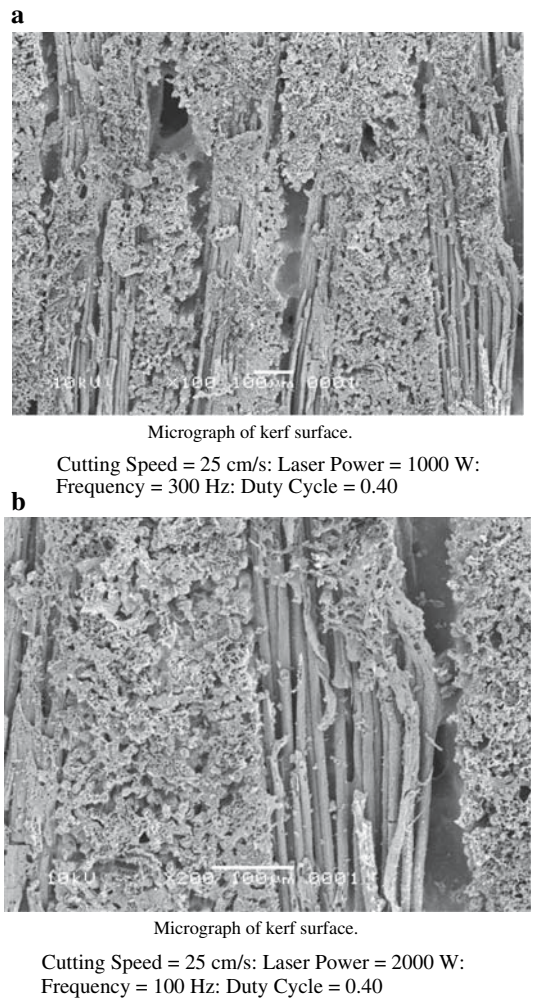

Fig. 8 SEM micrographs of kerf surfaces obtained at different cutting conditions. (a) Micrograph of kerf surface; Cutting Speed = 25 cm/s: Laser Power = 1000 W: Frequency = 300 Hz: Duty Cycle = 0.40; (b) Micrograph of kerf surface; Cutting Speed = 25 cm/s: Laser Power = 2000 W: Frequency = 100 Hz: Duty Cycle = 0.40

processing parameters are found to be very significant. This shows that the coupling effect of laser output power and cutting speed has a significant effect on the kerf width damage size. In some cases (at high-power intensity and low-cutting speed), the damage size becomes more than that of the kerf width size, which is particularly true at the bottom surface of the workpiece. In this case, the shielding gas, which is nitrogen, reaching the bottom of the workpiece through the kerf width does not have enough pressure to prevent oxidation reactions taking place in this region during the cutting process. Consequently, sideways burnings enhances the damage size in this region.

Figure 7 shows photographs of laser cuts surfaces. In general, laser cuts are reasonably good and sideways burning at the top surface of workpiece is not notable while some local char formation and some small-sideways burning are visible at the bottom surface. The main cause for sideways burning is the air molecules, which are left or trapped in the laminate structure during the sample preparation. Figure 8 shows the SEM micrographs of the cut cross section for two cutting conditions.

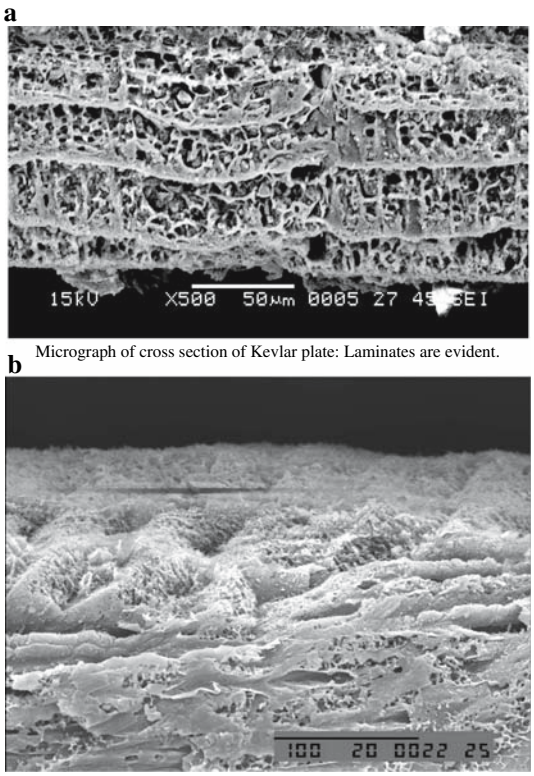

Fig. 9 SEM micrographs of plate and top-side view of kerf surfaces obtained at different cutting conditions; (a) Micrograph of cross section of Kevlar plate: Laminates are evident; (b) Micrograph of top-side view of Kerf surface: strias are evident; Cutting Speed = 25 cm/s: Laser Power = 1000 W: Frequency = 300 Hz: Duty Cycle = 0.40

Some small burnings at cut surfaces are visible, provided that the size of the sideways burning is considerably small. Figure 9 shows the cross section of the Kevlar plate and topside view of kerf surface. It is evident that the plate consists of laminates with thickness range of 25-50 µm. In addition, the spongy like structure of the laminate makes it easy to trap the air molecules during its preparation. This enhances the sideways burning at high-power intensity and low-cutting speeds. Moreover, striation formation is evident from the topside view of the kerf surface. However, the stria height is considerably small.

5. Conclusions

Laser cutting of Kevlar plates with different thicknesses is considered. Kerf width size, thermal efficiency of the cutting process and specific energy requirement for cutting are predicted for various cutting conditions. A statistical method using a factorial analysis is adopted to assess the effect of cutting parameters on the mean kerf width size and dimensionless damage size. It is found that kerf width size changes sharply for low-cutting speeds; however, as the cutting speed increases this variation becomes gradual. The kerf width size predicted agrees well with the experimental findings. Thermal efficiency increases with increasing workpiece thickness and cutting speed; however, it decreases with increasing laser output power. This is because of the high-power output, which is greater than the minimum power required for the cutting process. The specific energy requirement for cutting is reduced with increasing thickness. This is because of the amount of volume of the material removed from the kerf site, which increases with thickness for the same laser output power. *F*-test results indicate that the main effect of laser output power and cutting speed are very significant for mean kerf width size while laser pulse frequency are only significant. First order interactions of laser output power and cutting speed is found to have a significant effect on the mean kerf width size. This indicates that the coupling effect of laser output intensity and cutting speed influences the mean kerf width size significantly. In the case of dimensionless damage size, the main effects of all the cutting parameters are found to be very significant for the bottom surface of the cut section. The first order interaction of laser output power and cutting speed has a significant effect on the dimensionless damage size. Micrographs of the cut sections reveal that some locally distributed sideways burning occurs at the bottom surface of the workpiece. Nevertheless, the damage zone is considerably small.

Acknowledgments

The authors acknowledge the support of King Fahd University of Petroleum and Minerals Dhahran Saudi Arabia due to analytical tools for material characterization, and Karmetal due to laser cutting process.

References

1. B.S. Yilbas, Laser Cutting Quality Assessment and Thermal Efficiency Analysis, *J. Mater. Process. Technol.*, 2004, **155/156**, p 2106–2115
2. C.T. Pan and H. Hocheng, Prediction of Extent of Heat Affected Zone in Laser Grooving of Unidirectional Fiber-reinforced Plastics, *J. Eng. Mater. Technol.*, 1998, **120**, p 321–327
3. C.Y. Yue, G.X. Sui, and H.C. Looi, Effects of Heat Treatment on the Mechanical Properties of Kevlar-29 fibre, *Comp. Sci. Technol.*, 2000, **60**, p 421–427
4. S. Tandon, V.K. Jain, P. Kumar, and K.P. Rajurkar, Investigations into Machining of Composites, *Precision Eng.*, 1990, **12**(4), p 227–238
5. T. Hirogaki, E. Aoyama, H. Inoue, K. Ogawa, S. Maeda, and T. Katayama, Laser Drilling of Blind via Holes in Aramid and Glass/epoxy Composites for Multi-layer Printed Wiring Boards, *Composites: Part A*, 2001, **32**, p 963–968
6. A. Di Ilio and V. Tagliaferri, Thermal Damage in Laser Cutting of $(0/90)_{2s}$ Aramid/epoxy Laminates, *Composites*, 1989, **20**(2), p 115–119
7. J.W. Downing and J.A. Newell, Characterization of Structural Changes in Thermally Enhanced Kevlar-29 Fiber, *J. Appl. Polym. Sci.*, 2003, **91**, p 417–424
8. R.N. Walters, S. Hackett, and R.E. Lyon, Heats of Combustion of High Temperature Polymers, *Fire Mater.*, 2000, **24**, p 245–252
9. V. Tagliaferri, A. Di Ilio, and C.I. Visconti, Laser Cutting of Fibre-reinforced Polyesters, *Composites*, 1985, **16**(4), p 317–325
10. C.C. Chen and W. Cheng, Material Properties and Laser Cutting of Composites, *Int. SAMPE Tech. Conf.*, 1991, **23**, p 274–287
11. A.A. Cenna and P. Mathew, Analysis and Prediction of Laser Cutting parameters of Fibre Reinforced Plastics (FRP) Composite Materials, *Int. J. Mach. Tools Manuf.*, 2002, **42**(1), p 105–113
12. B.S. Yilbas, Investigation into Laser Cutting of Brush Bristles and Composite Plates, *Lasers Eng.*, 2003, **13**, p 155–165
13. F. Al-Sulaiman and B.S. Yilbas, Laser Treatment of a Carbon/carbon Reinforced Composite, *Lasers Eng.*, 2005, **15**(1-2), p 119–127
14. F.A. Al-Sulaiman, B.S. Yilbas, and M. Ahsan, CO_2 Laser Cutting of a Carbon/carbon Multi-lamelled Plain-weave Structure, *J. Mater. Process. Technol.*, 2006, **173**, p 345–351

15. M. Saeed Butt, N.A. Siddiqui, M. Zafar-uz-Zaman, and A. Munir, Study of Thermal and Mechanical Behavior of Chemically Stabilized Phenolic Based Composites, Proceeding of 2nd International Bhurban Conference on Applied Science and Technology, June 16–21, 2003, Bhurban, Pakistan, p 54–60
16. F. Al Sulaiman, Y.N. Al-Nassar, and E.M. Mokheimer, Prediction of the Thermal Conductivity of the Constituents of Fiber-Reinforced Composite Laminates: Voids Effect, *J. Comp. Mater.*, 2006, **40**(9), p 797–814
17. A. Kar, J.A. Rothenflue, and W.P. Latham, Scaling Laws for Thick-Section Cutting with a Chemical Oxygen-iodine Laser, *J. Laser Appl.*, 1997, **9**(6), p 279–286
18. O.L. Davies, *Design and Analysis of industrial experiments*. 1st ed., Longman Group Ltd, London, 1978
19. B.S. Yilbas, Study of Affecting Parameters in Laser Drilling of Sheet Metals, *Trans. ASME, J. Eng. Mater. Tech.*, 1987, **109**, p 282–287
20. B.S. Yilbas, J. Nickel, and A. Coban, Effect of Oxygen in Laser Cutting Process, *Mater. Manuf. Process.*, 1997, **12**(6), p 1163–1175
21. A.N. Shuaib, F.A. Al-Sulaiman, and F. Hamid, Machinability of Kevlar® 49 Composite Laminates while using Standard TiN Coated HSS Drills, *Mach. Sci. Technol.*, 2004, **8**(3), p 449–467